Proceedings of the 2007 IEEE
International Conference on Mechatronics and Automation
August 5 - 8, 2007, Harbin, China

Research on Biped Robot Gait in Double-support Phase

Liquan Wang, Zhiwei Yu, Feng He and Yu Jiao
College of Mechanical and Electrical Engineering
Harbin Engineering University
nantong street 145, Harbin 150001, China
yuyuefengting@eyou.com

Abstract - **This paper presented the gait of biped robot with actively driven toe-joint, established 9-link model of biped robot in sagittal plane, planned the gait with cubic spline interpolation and analyzed the change of supporting areas and the dynamic capability by comparing three different gaits in double-support phase. Basing on the theory of ZMP (Zero Moment Point) and simulating the gait in Matlab, it suggests that the gait of biped robot with actively driven toe-joint has many advantages over the others without it, such advantages include torques, angles and angle velocities of ankle joints and knee joints are smaller; and under the same condition of joints, the robot with toe-joint can realize larger walking step and quicker walking speed.**

Index Terms – Biped Robot; Toe-Joint; Gait planning; Double-support phase.

I. INTRODUCTION

As the rapid development of the technology in robots, biped robots can realize gaits such as walking on the ground, down and up inclined floor and stair, and some can even run (e.g. HRP-2LR[1], QRIO[2]). While researchers always design the thenar with structure of plane and then establish a leg with three DOF in coxa, one in knee and two in ankle [3], and the thenar of some passive biped robots contact the ground with point [4]. Such distribution of DOF restrains the gaits; in addition, the robot structure affects the dynamic capability directly which influence the utility of biped robot greatly. In order to improve humanoid robot walking gait, some scholars add more DOF of lower limbs, especially the toe-joint. To our knowledge the only humanoids robot with actively driven toe-joint are H7 [5], and there are only few robots with passive toe-joint (e.g. HRP-2TJ [6], WABIAN-2R [7]).

This paper adds actively driven toe-joint to traditional biped robot, establishes 9-links model, plans three different gaits using cubic spline interpolation and analyses the changes of supporting areas. Basing on ZMP theory and establishing the model in Matlab, this paper analyses the three different gaits during double-support phase, compares the disadvantages and advantages of each and suggests that gaits with actively driven toe-joint are better than the others without it; those advantages mainly include smaller angles, angle velocities and torques in ankle and knee joints in the same walking step and speed, that is to say under the same condition of joints, biped robot with actively driven toe-joints can walk with larger walking step and quicker walking speed.

II. ANALYSIS OF GAIT AND ESTABLISHMENT OF MODEL

A. Analysis of gait

Generally, the gaits in double-support phase include the two types, gait A and B. In gait A, as Fig.1a shows, the whole thenars contact the ground, when moving the upper body, the COG (Center Of Gravity) swifts from the rear supporting area to the front one accordingly to realize the exchange of supporting leg. In gait B, as Fig.1b shows, the rear heel leaves the ground after the front heel contacts the ground and then rotates with the tiptoe to make the front thenar contacts the ground, in such process, the COG switches from the rear supporting area to the front one to accomplish the change of supporting leg, and robots such as ASIMO use this gait [8].

This paper designs the gait of biped robot with actively driven toe-joint – gait C; as Fig.1c indicates, after the touch of front heel with the ground, the rear toe-joint rotates; when the whole front thenar contacts the ground, the rear thenar and toe rotate with the tiptoe to switch the supporting plane, and finally realize the exchange of supporting leg when COG from the back to the front. Humanoid robot H7 with actively driven toe-joint walking gait isn't like gait C, but like gait B, because its rear toe always parallel to the ground [9]. Robots with passive toe-joint also hardly walk like gait C, because the angle of passive toe-joint with spring-damp frame can't be driven and controlled easily.

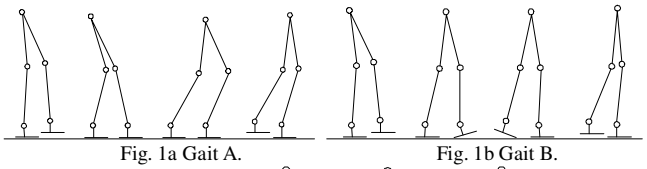

Fig. 1a Gait A. Fig. 1b Gait B.

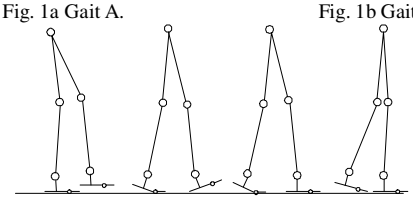

Fig. 1c Gait C.

B. Establishment of model

Usually, the DOF of biped robot is distributed as the following: three DOF in coax, one in knee and two in ankle,

and such distribution causes complex multi-link models. Generally, scholars establish model in the sagittal and lateral planes separately in order to simplify the model. This paper establishes 9-link model of the robot with toe-joint in sagittal plane as Fig.2 shows. Set the origin of inertial coordinate $\{o\}$ at the front heel, l_i is the length of bar i, m_i is the mass of bar i, l_{ic} is the barycenter position of bar i, and q_i is the generalized angle between the bar i and axis y. Bar 0 and 8 are toe, bar 1 and 7 are thenars, bar 2 and 6 are shank, bar 3 and 5 are thigh; while bar 4 is trunk. (x_h, y_h) is the position of coxa in coordinate $\{o\}$, α is the thenar angle, and θ_i is the every actual joint angle. Then we will have the following equations:

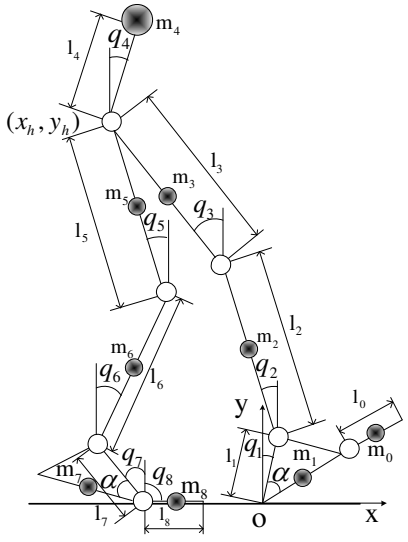

Fig. 2 Nine-link model.

$$\theta = Qq + Q' \tag{1}$$

In the equation:

$$Q = \begin{bmatrix} 1 & 0 & 0 & 0 & 0 & 0 & 0 & 0 \\ -1 & 1 & 0 & 0 & 0 & 0 & 0 & 0 \\ 0 & -1 & 1 & 0 & 0 & 0 & 0 & 0 \\ 0 & 0 & -1 & 1 & 0 & 0 & 0 & 0 \\ 0 & 0 & 0 & -1 & 1 & 0 & 0 & 0 \\ 0 & 0 & 0 & 0 & -1 & 1 & 0 & 0 \\ 0 & 0 & 0 & 0 & 0 & -1 & 1 & 0 \\ 0 & 0 & 0 & 0 & 0 & 0 & -1 & 1 \end{bmatrix}$$

$$Q' = \begin{bmatrix} \frac{\pi}{2} - \alpha & \alpha - \frac{\pi}{2} & 0 & 0 & 0 & 0 & \alpha - \frac{\pi}{2} & \pi - \alpha \end{bmatrix}^T$$

Lagrange dynamics equation of 9-links is:

$$\tau = M(q)\ddot{q} + C(q,\dot{q}) + G(q) + J^T F \tag{2}$$

In this equation τ is joint torques vector supplied by the driver, q is the generalized angles of joints vector, $C(q,\dot{q})$ is centrifugal moment, $G(q)$ is the moment of gravitation. While $M(q)$ is inertial matrix, F is external force, and J^T is Jacobian transpose.

III. Planning Gait And Analysis Of Stability

A. *Planning gait*

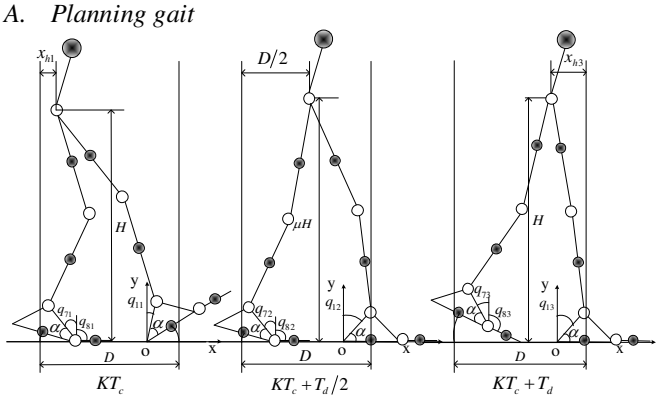

Fig. 3 Crucial stances.

The bipedal gait can be divided into double-support phase and single-support phase. Suppose T_c is one gait period, which includes the double-support time T_d and single-support time ($T_c - T_d$), and $\beta = T_d / T_c$, D is the length of one step. Analyse the three crucial stances in double-support phase. As Fig.3a shows the beginning status in the phase, the angle between l_1 and axis y is q_{11}, the angle between l_7 and axis y is q_{71}, and the angle between l_8 and axis y is q_{81}. The position of coxa is determined by x_{h1} and H, the position of rear heel is determined by variables q_{71}, q_{81}, l_7 and l_8, and the position of front heel is determined by q_{11} and l_1. Fig.3b shows the middle stance of double-support phase; the angle between l_1 and axis y is q_{12}, the angle between l_7 and axis y is q_{72}, and the angle between l_8 and axis y is q_{82}; the position of coxa is determined by $D/2$ and $\mu \cdot H$, the position of rear heel is determined by the variable q_{72}, q_{82}, l_7 and l_8, and the position of front heel is determined by q_{12} and l_1. Fig.3b shows the final stance of double-support phase; the angle between l_1 and axis y is q_{13}, the angle between l_7 and axis y is q_{73}, and the angle between l_8 and axis y is q_{83}; the position of coxa is determined by x_{h3} and H, the position of rear heel is determined by the variable q_{73}, q_{83}, l_7 and l_8,

and the position of front heel is determined by q_{13} and l_1. Due to the periodicity of the whole gait and alternately exchange of the back and front leg, this paper uses cubic spline interpolation to approach the position of coxa, ankle and angle variables q_1, q_7 and q_8 at crucial status in order to make sure the trajectory of first and second derivative continuity, and the detail will not expatiate. It supposes the origin of inertial coordinate $\{o\}$ at the heel point $(KD,0)$ after K steps; the initial time of double-support phase is KT_c, then the position of coxa $(X_h(t),Y_h(t))$, rear ankle $(X_{ra}(t),Y_{ra}(t))$ and front ankle $(X_{fa}(t),Y_{fa}(t))$ at the crucial stances can be expressed as:

$$X_h(t)=\begin{cases}(k-1)D+l_1\cos(\alpha)+x_{h1} & t=kT_c\\ (k-1)D+l_1\cos(\alpha)+D/2 & t=kT_c+T_h\\ kD+l_1\cos(\alpha)-x_{h3} & t=kT_c+T_d\\ kD+l_1\cos(\alpha)+x_{h1} & t=(k+1)T_c\end{cases} \tag{3}$$

$$Y_h(t)=\begin{cases}H & t=kT_c\\ uH & t=kT_c+T_h\\ H & t=kT_c+T_d\\ H & t=(k+1)T_c\end{cases} \tag{4}$$

$$X_{ra}(t)=\begin{cases}(k-1)D+l_7(2\cos(\alpha)-\sin(q_{71}))+l_8(1+\sin(q_{81})) & t=kT_c\\ (k-1)D+l_7(2\cos(\alpha)-\sin(q_{72}))+l_8(1+\sin(q_{82})) & t=kT_c+T_h\\ (k-1)D+l_7(2\cos(\alpha)-\sin(q_{73}))+l_8(1+\sin(q_{83})) & t=kT_c+T_d\\ (k+1)D+l_1(-\sin(q_{11})) & t=(k+1)T_c\end{cases} \tag{5}$$

$$Y_{ra}(t)=\begin{cases}l_7\cos(q_{71})-l_8\cos(q_{81}) & t=kT_c\\ l_7\cos(q_{72})-l_8\cos(q_{82}) & t=kT_c+T_h\\ l_7\cos(q_{73})-l_8\cos(q_{83}) & t=kT_c+T_d\\ l_1\cos(q_{11}) & t=(k+1)T_c\end{cases} \tag{6}$$

$$X_{fa}(t)=\begin{cases}kD+l_1(-\sin(q_{11})) & t=kT_c\\ kD+l_1(-\sin(q_{12})) & t=kT_c+T_h\\ kD+l_1(-\sin(q_{13})) & t=kT_c+T_d\\ kD+l_7(2\cos(\alpha)-\sin(q_{71}))+l_8(1+\sin(q_{81})) & t=(k+1)T_c\end{cases} \tag{7}$$

$$Y_{fa}(t)=\begin{cases}l_1\cos(q_{11}) & t=kT_c\\ l_1\cos(q_{12}) & t=kT_c+T_h\\ l_1\cos(q_{13}) & t=kT_c+T_d\\ l_7\cos(q_{71})-l_8\cos(q_{81}) & t=(k+1)T_c\end{cases} \tag{8}$$

The variables q_{1i}, q_{7i} and q_{8i} in these equations are the cubic interpolation of q_1, q_7 and q_8 correspondingly.

When analysing those three different gaits, it suppose the value of q_{1i}, q_{7i} and q_{8i} correspondingly. Details are shown in table I.

According to the geometric restriction of bipedal motion, the adjustable parameters showed above are fit to the following restrictions: $|x_{h1}|\le 0.5D$, $|x_{h3}|\le 0.5D$, $0\prec\beta\prec 1$, $0\le\mu\le 1$, $\alpha-\pi/2\prec\varphi_1\prec 0$, $\phi_1\prec\psi_1\prec\pi/2-\alpha$, $-\pi/2\prec\gamma\prec-\pi$. According to the trajectory of coxa and ankle approached by cubic spline interpolation, the trajectories of knee position and rotating angles of different joints can be easily get and are ignored here.

TABLE I

q_{1i}, q_{7i}, q_{8i} OF THREE GAITS rad

	Gait A	Gait B	Gait C
q_{11}	$\alpha-\pi/2$	φ_1	φ_1
q_{12}	$\alpha-\pi/2$	$\alpha-\pi/2$	$\alpha-\pi/2$
q_{13}	$\alpha-\pi/2$	$\alpha-\pi/2$	$\alpha-\pi/2$
q_{71}	$\pi/2-\alpha$	$\pi/2-\alpha$	$\pi/2-\alpha$
q_{72}	$\pi/2-\alpha$	ψ_1	ψ_1
q_{73}	$\pi/2-\alpha$	ϕ_1	ϕ_1
q_{81}	$-\pi/2$	$-\pi/2$	$-\pi/2$
q_{82}	$-\pi/2$	$\psi_1+\alpha-\pi$	$-\pi/2$
q_{83}	$-\pi/2$	$\phi_1+\alpha-\pi$	γ

B. *Analysis of stability*

The changing of supporting areas are different in the three gaits as Fig.4 shows; axis X is moving direction, axis t is time, C_α is $\cos\alpha$, the area of 2 and 3 are the time during double-support phase, while 1 and 4 are the time during single-support phase. The areas of A, B, C, D and E reflect the gait A; the areas of A, C and D reflect the gait B; and area C and D reflect gait C.

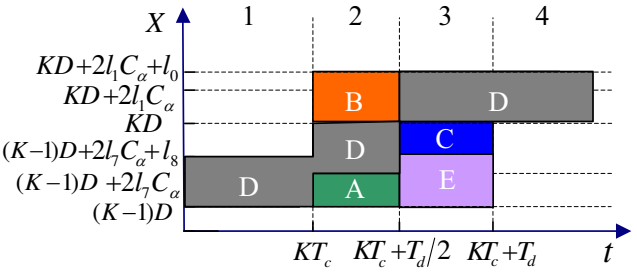

Fig. 4 Support area.

Generally, adopt the criterion of ZMP to judge the stability of gait, which suggests that the step is stable if the ZMP is within the supporting area during walking. And the equation is shown as following:

$$X_{ZMP}=\frac{\sum m_i y_{ic}\ddot{x}_{ic}-\sum(m_i(\ddot{y}_{ic}+g)x_{ic}+I_{ic}\ddot{\theta}_i)}{-\sum m_i(\ddot{y}_{ic}+g)} \quad (9)$$

x_{ic} and y_{ic} are the COG position of bar i; $\ddot{x}_{ic}$ and $\ddot{y}_{ic}$ are the COG accelerate of bar i; I_{ic} is rotate inertia of bar i,and $\ddot{\theta}_i$ is angle acceleration.

IV. Gait Simulation

9-link model with toe-joint was established in Matlab as Fig.5 shows, and then simulated according to the structural parameters of biped robot HEUBR_1 which are listed in Tab. II and Tab. III.

TABLE II

LINKS' LENGTH mm

l_0	l_1	l_2	l_3	l_4	l_5	l_6	l_7	l_8
50	200	500	500	200	500	500	200	50
l_{0c}	l_{1c}	l_{2c}	l_{3c}	l_{4c}	l_{5c}	l_{6c}	l_{7c}	l_{8c}
25	100	250	250	200	250	250	100	25

TABLE III

DISTRIBUTED MASS kg

m_0	m_1	m_2	m_3	m_4	m_5	m_6	m_7	m_8
0.5	1	4	5	6	5	4	1	0.5

In order to analyse different gaits under the same status, suppose T_c is 2 seconds, β is 0.5, μ is 1 and α is 0.4636. Simulate gait A when $D=0.3$m, $H=1.0$m and $x_{h1}=x_{h3}$=0.0m, as Fig.6a shows that the trajectory of ZMP is within the supporting area, so this gait is stable; when $H=0.8$m, $x_{h1}=x_{h3}=-0.05$m and $D=0.5$m, as Fig.6b shows gait A is still stable. Simulate gait B when $D=0.5$m, $H=0.95$m and $x_{h1}=x_{h3}$=0.05m, as Fig.6c shows the trajectory of ZMP is within the supporting area, and according to the theory of ZMP this gait is stable. Simulate gait C when $D=0.5$m, $H=0.95$m and $x_{h1}=x_{h3}$=0.05m, as Fig.6b shows this gait is also stable.

Fig.7a is stick figure about one stable state of gait A ($D=0.3$m); Fig.7b is stick figure about one stable state of gait A($D=0.5$m); Fig.7c shows one stable state of gait B($D=0.5$m) and Fig.7d shows one stable state of gait C($D=0.5$m); Fig.8a, fig.8b, fig.8c and fig.8d show the trajectory of angle velocities of part joints in different gaits suggested above (gait A when $D=0.3$m, gait A when $D=0.5$m, gait B and gait C)； while fig.9a, fig.9b, fig9c and fig.9d indicate the driving torque curves of part joints to the gaits suggested above (gait A when $D=0.3$m, gait A when $D=0.5$m, gait B and gait C). According to fig.7a, fig.7b, fig8a, fig.8b, fig.9a and fig.9b, in gait A, when D is 0.5m, the joint angles, angle velocities and driving torques are much larger than these in the gait when D is 0.3m, especially the joint angles and angle velocities of ankle and knee joints, and the knee joint torques; According to fig.7b, fig.7d, fig8b, fig.8d, fig.9b and fig.9d, the joint angles, angle velocities and joint torques in gait C are much smaller than these in gait A ($D=0.5$m),especially the joint angles and angle velocities of ankle and knee joints, and the knee joint torques; According to fig.7c, fig.7d, fig8c, fig.8d, fig.9c and fig.9d, angle of every joint in gait C and B are much same, but the knee angle velocity and ankle torque of rear supporting leg in gait C are smaller than these in gait B, and in gait C, the change of angle velocity at rear ankle is more smooth.

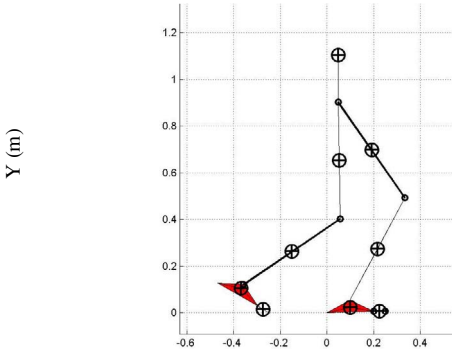

Fig. 5 Simulated model.

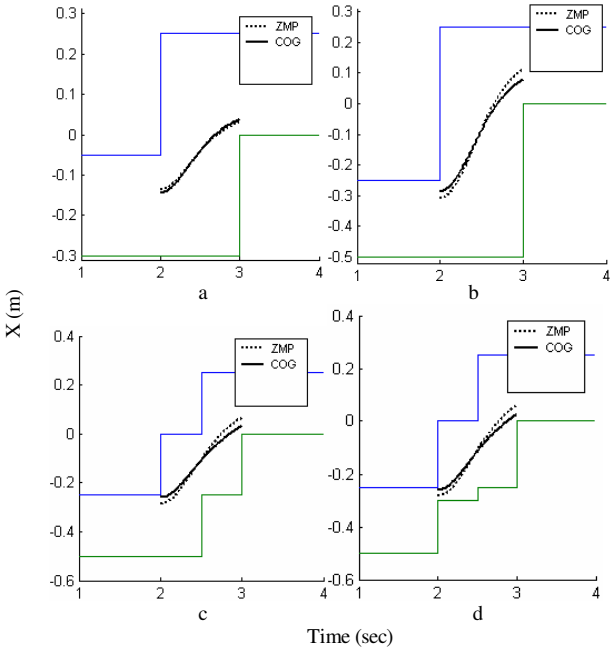

Fig. 6 ZMP and COG trajectory.

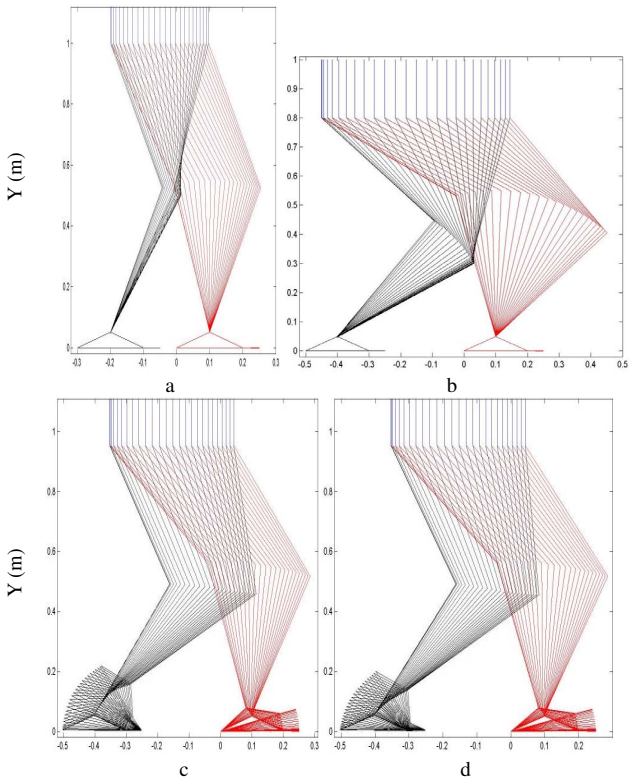

Fig. 7 Stick figure.

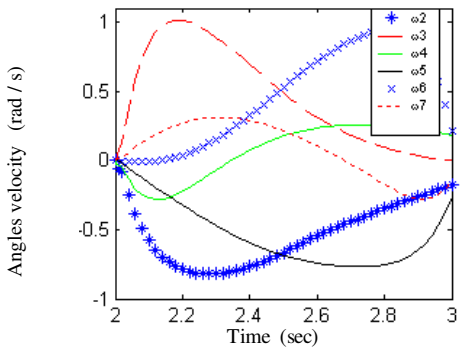

Fig. 8a Angles velocity in gait A ($D = 0.3$m).

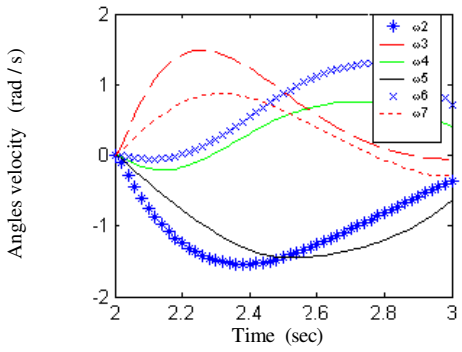

Fig. 8b Angles velocity in gait A ($D = 0.5$m).

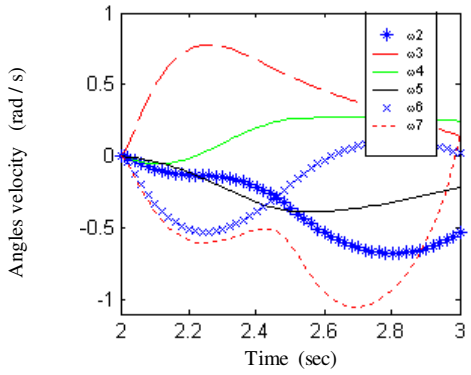

Fig. 8c Angles velocity in gait B ($D = 0.5$m).

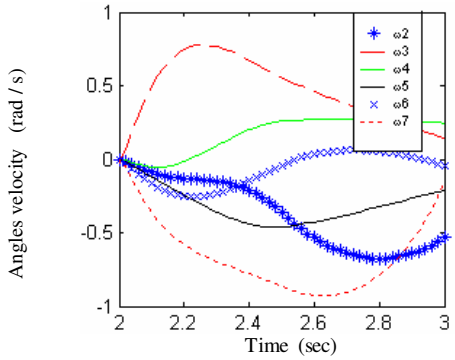

Fig. 8d Angles velocity in gait C ($D = 0.5$m).

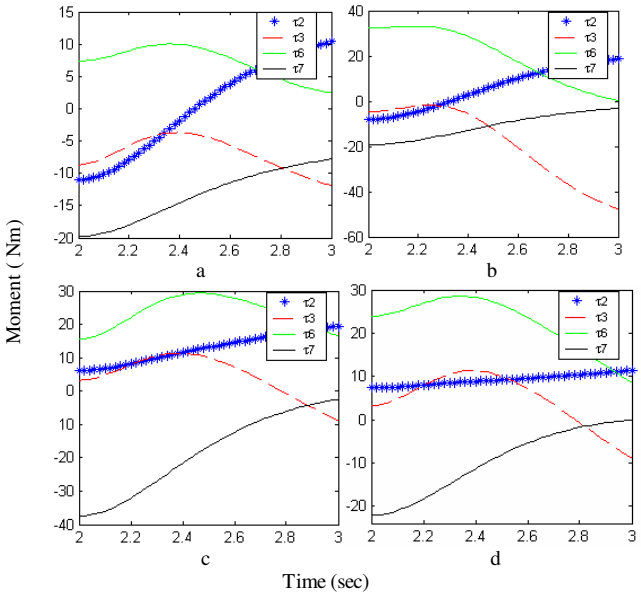

Fig. 9 Joints driving moment track.

V. Conclusion

According to the research, the angles, angle velocities and joint torques increase as the growing of walking step in gait A; when compared with gait A at the same step, gait C has much smaller angles, angle velocities and joint torques; when compared with gait B at the same step, the angle

velocities of knee and the torque at ankle joint of the rear supporting leg in gait C are smaller, in addition, the change of velocity at ankle joint of the rear supporting leg in gait C is more smooth. In sum, the humanoid gait like gait C with actively driven toe-joint has some merits as compared to the others without toe-joint, under the same condition of joints, the robot with toe-joint can realize larger walking step and quicker walking speed.

ACKNOWLEDGMENT

Finally, the authors would like to thank to the Scientific Research Fund of the Harbin Engineering University for their financial support.

REFERENCES

[1] S. Kajita, T.Nagasaki, and K.Kaneko,et al, "A Running Controller of Humanoid Biped HRP-2LR," *Proceedings of the 2005 IEEE International Conference on Robotics and Automation, Barcelona, Spain*,pp.618-624 April 2005.

[2] K.Nagasaka, Y. Kuroki, and S. Suzuki, et al, "Integrated Motion Control for Walking, Jumping and Running on a Small Bipedal Entertainment Robot," *Proceedings of the 2004 IEEE International Conference on Robotics & Automation, New Orleans, LA,* pp. 3189-3194, April 2004.

[3] Y.-M. Li, "Foreign Status of Humanoid Robot," *Robot,* vol. 27, no. 6, pp.561-568, November 2005.

[4] S.-H. Hyon and T. Emura, "Symmetric Walking Control: Invariance and Global Stability," *Proceedings of the 2005 IEEE International Conference on Robotics and Automation, Barcelona, Spain,* pp. 1143-1152, April 2005.

[5] K. Nishiwaki, S. Kagami, and Y. Kuniyoski, et al, "Toe joints that enhance bipedal and fullbody motion of humanoid robots," *Proceedings of the 2002 IEEE International Conference on Robotics & Automation, Washington. DC, USA,* pp.3105-3110. May 2002.

[6] R. Sellaouti, O. Stasse, and S. Kajita, et al, "Faster and Smoother Walking of Humanoid HRP-2 with Passive Toe joints," *Proceedings of the 2006 IEEE/RSJ International Conference on Intelligent Robots and Systems, Beijing, China,* pp.4909-4914,October 2006.

[7] Y. Ogura, K. Shimomura, and H. Kondo, et al, "Human-like Walking with Knee Stretched, Heel-contact and Toe-off Motion by a Humanoid Robot," *Proceedings of the 2006 IEEE/RSJ International Conference on Intelligent Robots and Systems, Beijing, China,* pp.3976-3981,October 2006.

[8] J.Chestnuut, M.Lau, and G.Cheung, et al, "Footstep Planning for the Honda ASIMO Humanoid," *Proceedings of the 2005 IEEE International Conference on Robotics and Automation, Barcelona, Spain*, pp.629-634, April 2005.

[9] K. Nishiwaki, S. Kagami, and J. Kuffner, et al, "Humanoid 'JSK-H7': Research Platform for Autonomous Behavior and Whole Body Motion," *Proceedings of the Third IARP International Workshop on Humanoid and Human Friendly Robotics, Tsukuba, Japan,* pp.2-9, December 2002.